

# Using Thermally Stimulated Current (TSC) to Investigate Disorder in Micronized Drug Substance Produced at Different Milling Energies

Rachel Forcino · Jeffrey Brum · Marc Galop · Yan Sun

Received: 18 May 2010 / Accepted: 23 July 2010 / Published online: 10 August 2010  
© Springer Science+Business Media, LLC 2010

## ABSTRACT

**Purpose** To investigate the use of thermally stimulated current (TSC) to characterize disorder resulting from micronization of a crystalline drug substance. Samples processed at different milling energies are characterized, and annealing studied.

**Methods** Molecular mobility in micronized drug substance was studied using TSC and compared to results from differential scanning calorimetry (DSC). The micronized drug substance TSC spectra are compared to crystalline and amorphous references.

**Results** TSC shows distinct relaxation modes for micronized material in comparison to a single weak exotherm observed with DSC. Molecular mobility modes are unique for micronized material compared to the amorphous reference indicating physically distinct disorder compared to phase-separated amorphous material. Signals are ascribed as arising from crystal defects. TSC differentiates material processed at different milling energies showing reasonable correlation between the AUC of the  $\alpha$ -relaxation and micronization energy. The annealing process of crystal defects in micronized drug appears to proceed differently for  $\alpha$  and  $\beta$  relaxations.

**Conclusions** TSC proves sensitive to the crystal defects in the micronized drug substance studied here. The technique is able to differentiate distinct types of disorder and can be used to characterize noncrystalline regions arising from milling processes which are physically distinct from amorphous material.

**KEY WORDS** annealing of surface disorder · crystal defects · micronization energy · non-crystalline content · thermally stimulated current (TSC)

## INTRODUCTION

Solid-state molecular mobility has been studied via numerous techniques, including differential scanning calorimetry (DSC), isothermal microcalorimetry, solid-state nuclear magnetic resonance (SSNMR) spectroscopy, and dielectric techniques, such as dynamic dielectric spectroscopy and thermally stimulated current spectroscopy (TSC) (1). Dielectric techniques provide better sensitivity to weak molecular relaxation processes, including glass transitions ( $T_g$ ) and sub- $T_g$  relaxations (2,3). TSC can be used to investigate relaxations which are responsible for non-cooperative rotational motions ( $\beta$ -relaxations) as well as cooperative rotational and translational motions that occur at the lower temperature range of the glass transition ( $\alpha$ -relaxations) (4–8). This technique can also experimentally resolve broad global relaxations into individual components using fractional polarization (9,10).

In pharmaceutical production, milling processes are a common operation for particle size reduction used to improve drug substance dissolution, processability, or bioavailability. Milling processes in general may result in the generation of metastable or amorphous phases; however, the specific mechanisms responsible for these solid-state transformations are complex and continue to be areas for investigation (11). Micronization is a common milling procedure where size attrition is accomplished via high-speed particle-particle collisions. Structural changes and mechanical stress resulting from micronization can be associated with lattice defects and degradation of crystalline structure (12). Depending on the amount of energy imparted

R. Forcino · J. Brum (✉) · Y. Sun  
Physical Properties Analytical Sciences, Pharmaceutical Development  
GlaxoSmithKline Pharmaceuticals  
1250 S. Collegeville Road  
Collegeville, Pennsylvania 19426, USA  
e-mail: jeffrey.brum@gsk.com

M. Galop  
Early Development Group, Pharmaceutical Development  
GlaxoSmithKline Pharmaceuticals  
Collegeville, Pennsylvania, USA

and the specific mechanical properties of the material, phase-separated regions of amorphous material may result where a volume of the particle has lost the symmetry aspects associated with the crystalline state and an isotropic configuration of molecules results (13,14). Although the standard for establishing crystallinity in pharmaceutical powders is X-ray powder diffraction (XRPD), low levels of lattice defects or amorphous phases imbedded in otherwise crystalline micronized particles can be difficult to detect or quantify effectively as the technique primarily interrogates bulk domains—crystalline or disordered—of the sample (15,16). TSC has demonstrated the sensitivity to detect small amounts (~1%) of an amorphous phase because the TSC relaxation signal comes only from the amorphous phase (15).

As discussed above, the mechanically induced stress of micronization may not result in the transformation to a true amorphous phase. The main objective of this study was to characterize regions of disorder that result from micronization, which are distinct from a true phase-separated amorphous material. We found TSC to be a valuable technique towards this end and compare results to those obtained from DSC. Materials processed with different milling energies were also examined to evaluate TSC responses to materials which may contain varying levels of non-crystalline content. The final objective was to monitor and characterize the aging process of disordered regions present in micronized drug substance as a function of storage conditions.

## MATERIALS & METHODS

### Materials

The compound investigated in this study is a crystalline anhydrous HCl salt (Compound 1) which is formulated as an IR tablet. The material is micronized before the formulation process for the purpose of improving clinical exposure and content uniformity in the tablets. The non-micronized material was utilized as the crystalline reference material. Additional samples employed in this work were an amorphous reference material prepared by ball milling and samples prepared via milling at different micronization energies. They are described below.

The amorphous reference sample was prepared using a Retsch mixer mill (MM 2000) equipped with stainless steel grinding jar and balls (diameter 10 mm). The material was ball milled at room temperature for 25 min. The process was run in 5 min intervals, and the interior of the grinding jar was scraped of powder using a stainless steel spatula between each milling cycle. Following the milling process, additional grinding was applied to the sample using hand processing via mortar and pestle.

Micronized material analyzed in this study was processed over a range of milling energies generating drug substance samples with potentially varying levels of non-crystalline content, although particle size ranges for the sample set are comparable. The milling of the compound in this investigation was done using a spiral jet mill where the particle size reduction is primarily through particle-particle collisions. The process is driven through the use of high pressure nitrogen gas which creates the gas kinetic energy required for particle size reduction. The particle size reduction efficiency is controlled through material feeding rate, venturi pressure and grinding pressure. For this investigation, the material feed rate was varied in the range of 15 to 50 kg/hr, the venturi gas pressure was varied from 40 to 80 psi, and the grinding pressure was varied from 40 to 80 psi. The milling energy is a computed value based on the control level of these three parameters and ranged in this work from 90 to 450 kJ/kg.

### Thermally Stimulated Current

TSC measures the electrical current induced by temperature-activated relaxation of molecular dipoles in response to an applied static electric field. Generally, a thermally stimulated depolarization current (TSDC) method is used to study molecular relaxations. The first step of TSDC includes polarization of the sample at a specific temperature to orient mobile molecular dipoles, then the temperature is lowered to where molecular mobility is reduced. When the electric field is subsequently removed, the oriented dipoles are immobile, and the polarization trapped. The temperature is then ramped, and the current recorded. The micronized drug substance investigated in this work demonstrates thermal memory in TSDC runs; thus, the relaxation modes are not reversible. TSC work on pharmaceutical powders is limited; however, thermal memory in organic materials does not appear to be generally observed (2,3,7).

The alternative approach employs thermally stimulated polarization current (TSPC). The TSPC experiment starts at a low temperature where molecular mobility is reduced. The electric field is maintained throughout the experiment. As the temperature is ramped and the molecular mobility increases, the dipoles within the molecules orient in the field and produce a polarization current which is recorded. TSPC analyses were performed on powder samples hand-pressed into disks of about 1 mm thickness. The disk was placed between a pivot electrode and base plate of a TherMold TSC/RMA 9000 spectrometer with an insulating film of polyimide (Kapton®) inserted between the sample disk and base plate. Thus, the current that is measured characterizes segmental molecular motions in disordered regions, and not conduction current. All tests presented in this article were performed using polarization

mode. The sample was cooled to  $-50^{\circ}\text{C}$ , then an electric field was applied (127–141 V). The sample was ramped at  $7^{\circ}\text{C}/\text{min}$  to  $180^{\circ}\text{C}$ , and the current generated due to the polarization of dipoles was recorded. The current values reported are normalized for sample weight, area, and electric field applied during analysis.

### Differential Scanning Calorimetry

DSC analyses were performed on a TA Q2000 instrument. Approximately 2 mg of sample were weighed into an aluminium pan and loosely covered with the lid. Samples were heated at a rate of  $10^{\circ}\text{C}/\text{min}$  to  $300^{\circ}\text{C}$ . Alternate heating rates were also explored.

### X-Ray Powder Diffractometry

XRPD patterns were collected on a Panalytical X'Pert Pro Diffractometer using  $\text{Cu K}\alpha$  radiation operated in reflection mode to capture the  $2\theta$  range of  $2^{\circ}$  to  $35^{\circ}$ .

### Gravimetric Vapor Sorption

Gravimetric vapor sorption (GVS) data was collected with a Surface Measurements Systems DVS-1000 instrument. Moisture sorption isotherms were collected at 25 and  $40^{\circ}\text{C}$  over the range of 0 to 90 % relative humidity (RH) in increments of 5 % RH.

## RESULTS AND DISCUSSION

### Characterization of Disorder Post Micronization

Figure 1 shows a section of the XRPD pattern between  $4^{\circ}$  and  $35^{\circ}$   $2\theta$  of Compound 1 taken before and after micronization. No gross changes indicative of bulk levels of amorphous material (e.g. baseline deflection) are evident. Shown in Fig. 2 is the same pair of samples run by DSC

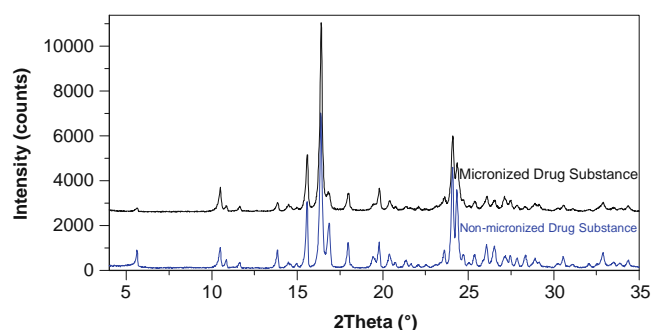


**Fig. 1** XRPD patterns for Compound 1 before and after micronization. The diffractograms are comparable indicating that no bulk amorphous content has formed as a result of micronization.

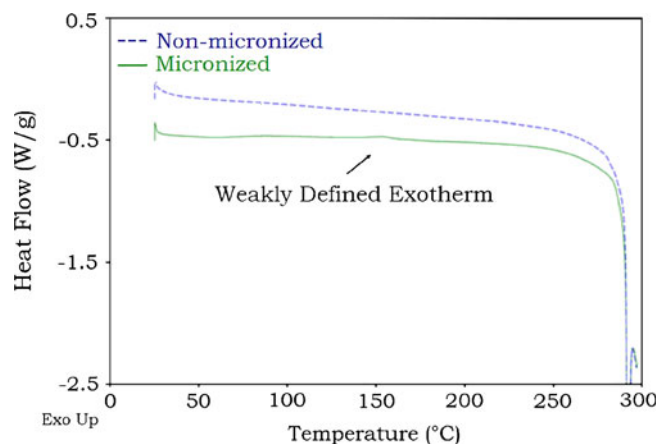


**Fig. 2** DSC thermograms for Compound 1 before and after micronization acquired at  $10^{\circ}\text{C}/\text{min}$ . The arrow indicates the location of a very weak and poorly defined exotherm, which is discussed more thoroughly in the text.

using the conditions noted above. At the vertical resolution shown, no clear differences are noted in the thermograms before and after micronization. As such, the micronized samples are comparable to that of the non-micronized sample in that neither displays any significant thermal event prior to the onset of decomposition at  $\sim 275^{\circ}\text{C}$ . There is in fact a very weak exothermic event in micronized material indicated in Fig. 2 which displays a poorly defined onset around  $140^{\circ}\text{C}$ . The feature will be discussed further below. Close examination of this thermogram below  $100^{\circ}\text{C}$  indicates the possible presence of additional weak features. For micronized samples, these features are not reproducible and are ascribed to baseline noise/drift.

Although no significant thermal signature associated with non-crystalline material is produced in the DSC analysis of micronized material, evidence of disorder is easily noted in the TSPC traces. An overlay of the TSPC results for non-micronized drug substance and its corresponding micronized batch is presented in Fig. 3. It

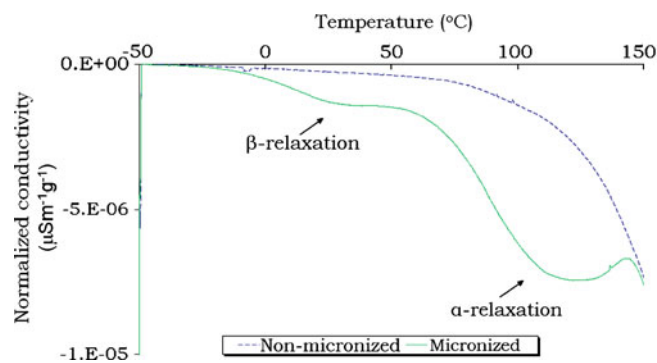


**Fig. 3** TSPC thermograms for Compound 1 before and after micronization acquired with the instrumental conditions described in the text.  $\beta$  and  $\alpha$  relaxation modes are present in the thermogram of the micronized sample.

is clearly seen from this overlay that micronized drug substance exhibits molecular relaxations below 150°C in the form of negative peaks or shoulders that are not observed in unprocessed material. Two well-separated modes of mobility are present in the micronized batch, the  $\beta$ -relaxation attributable to non-cooperative motion in the temperature range of  $-20$ – $50$ °C, and the  $\alpha$ -relaxation due to cooperative movements in the range of  $80$ – $150$ °C (4).

To further investigate the nature of the non-crystalline material resulting from micronization, and responsible for the observed TSPC relaxations, an amorphous reference material was prepared as described above and analyzed. This reference would be representative of a truly phase-separated amorphous region generated by the process. The XRPD pattern of the amorphous reference sample measured between  $2^\circ$  and  $35^\circ 2\theta$  is shown in Fig. 4a and confirms that long-range order has been eliminated. As shown in Fig. 2, post-micronization Compound 1 exhibits negligible changes detectable by XRPD compared to input material. The DSC thermogram of the amorphous reference shown in Fig. 4b displays a broad dehydration endotherm beginning near ambient and extending past

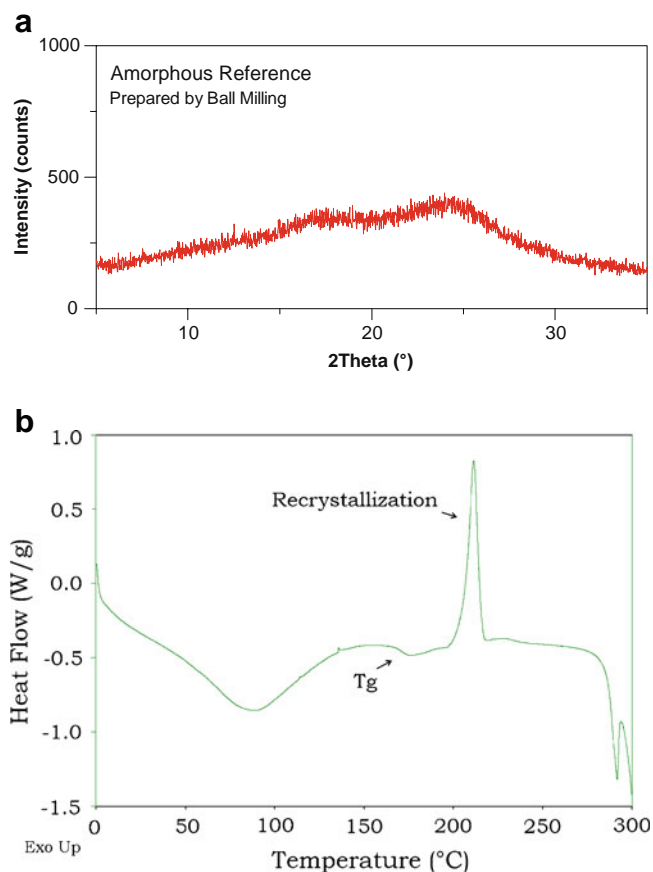


**Fig. 4** **a** XRPD pattern for the amorphous reference acquired between  $2^\circ$  and  $35^\circ 2\theta$ , and **b** DSC thermogram for the amorphous reference where the  $T_g$  and recrystallization features are clearly observed.

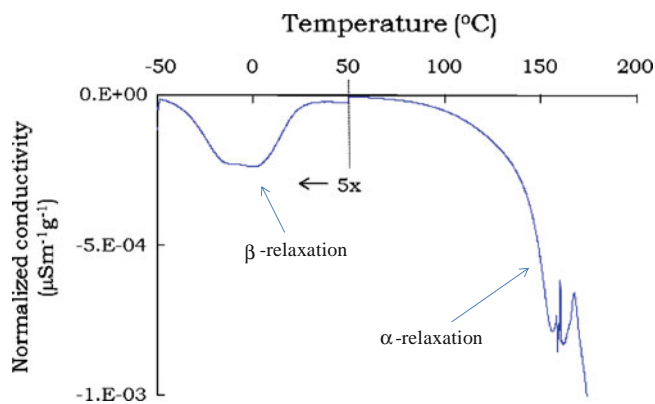


**Fig. 5** TSPC thermogram for the amorphous reference acquired with the instrumental conditions described in the text.  $\beta$  and  $\alpha$  relaxation modes are present in the thermogram; however, they occur in different locations compared to the micronized sample. Below  $50$ °C the normalized conductivities are presented at 5x the measured value to expand the  $\beta$ -relaxation signal.

$100$ °C. The endotherm, not present in the non-micronized or micronized samples (see Fig. 2), results from the enhanced ability of the amorphous material to absorb ambient moisture. A glass transition at  $170$ °C is clearly visible. This is followed by a recrystallization exotherm with an onset temperature of  $200$ °C.

TSPC results for the prepared amorphous reference sample are presented in Fig. 5; this sample also demonstrates two relaxation modes. The  $\beta$ -relaxation is observed in the range of  $-50$ – $50$ °C. The  $\alpha$ -relaxation appears in the temperature range of  $140$ – $165$ °C, consistent with cooperative motion associated with the  $T_g$  observed in the DSC trace. In Fig. 6 the amorphous reference TSPC is overlaid with the trace obtained from the micronized sample presented in Fig. 3. It is clear that the features appearing in each sample arise in different temperature ranges. The  $\beta$ -relaxation in the amorphous sample has an onset approx-

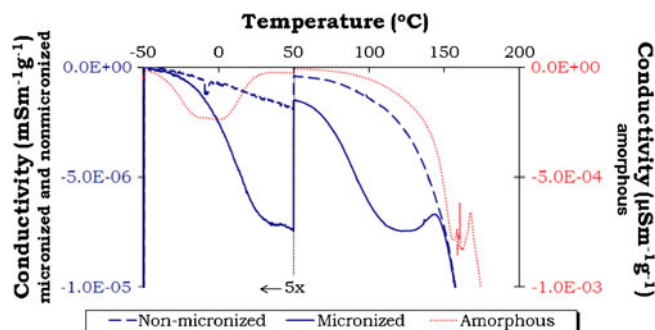


**Fig. 6** Overlay of TSPC spectra for micronized Compound 1, unprocessed reference, and the amorphous reference. The y axes are different for the unprocessed reference and micronized sample (left axis) and amorphous reference (right axis) traces. Below  $50$ °C the normalized conductivities are presented at 5x the measured value to expand the  $\beta$ -relaxation.

imately 30°C lower in temperature as compared to that observed in the micronized sample. For the  $\alpha$ -relaxation, the onset is observed approximately 60°C higher for the amorphous reference as compared to the micronized sample. These results clearly indicate that the non-crystalline material arising as a result of micronization is physically distinct from phase-separated amorphous material. This suggests that micronized material cannot be simply modeled as a mixture of purely crystalline and purely amorphous phases, but rather the disordered regions are perhaps more appropriately seen as containing a range of lattice disorder. In other words, the data show that the disorder-induced post-micronization is consistent with a “one-state model” as opposed to the “two-state model” (13,16). Similar observations were recently reported by Charmathy and Pinal, who investigated cryomilled samples of Griseofulvin and Felodipine using TSPC and noted material consistent with what they describe as crystal defects as opposed to an amorphous phase (12).

The observed difference in the  $\beta$ -relaxation temperatures suggests that less activation energy is required to initiate local non-cooperative motion in the amorphous reference sample as compared to the micronized sample. The magnitude of the relaxation was significantly greater in the amorphous reference, attributable to a larger quantity of molecules capable of non-cooperative motion. Molecular mobility is observed in the samples due to disorder generated during micronization and ball-milling processes, and it is clear that distinct types of disorder are associated with the  $\beta$ -relaxation.

The  $\alpha$ -relaxation is observed as a peak or shoulder on the polarization curve, after which polarization of ordered molecules is responsible for the rapid increase in current. The  $\alpha$ -relaxation for micronized drug substance is broader and occurs at a lower temperature range compared to the amorphous reference. The shift in the location and magnitude of the transition confirms again that the observed  $\alpha$ -relaxation for the micronized drug substance arises from disordered material which is physically distinct from that of the amorphous reference material. The  $\alpha$ -relaxation observed in the amorphous reference material is attributable to the cooperative motion of molecules during the glass transition. A  $T_g$  was clearly observed in the DSC thermogram for the amorphous reference; however, the micronized material shows a different thermal profile, and no  $T_g$  is observed. The  $\alpha$ -relaxation in the micronized material is consistent with a cooperative motion event in advance of the very weak exotherm observed in the DSC (described in greater detail below) which can be associated with the recrystallization/healing of crystal defects.

Figure 7 contrasts DSC thermograms for amorphous and micronized samples at expanded vertical resolution as compared to Fig. 3. In this trace, the very shallow, broad,

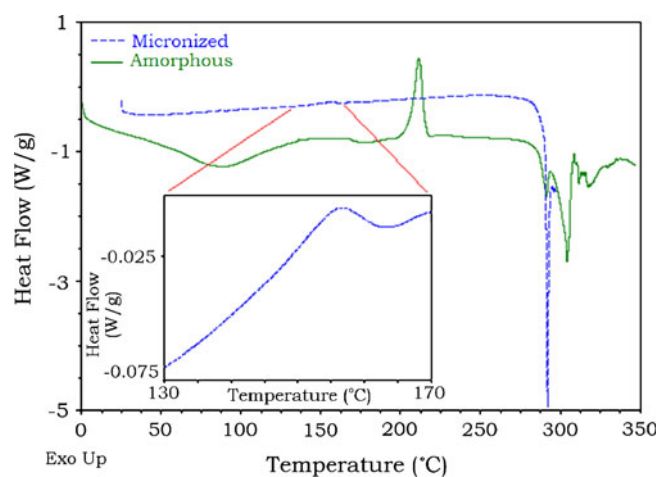


**Fig. 7** DSC trace for micronized Compound I overlaid with the amorphous reference. The window displays an expanded region showing the weak exotherm visible in the DSC trace of micronized materials; this feature has a poorly defined onset and poor reproducibility.

and poorly reproducible exotherm present in the micronized sample is seen between 140 and 160°C, substantially lower in temperature than that of the  $T_g$  observed at 170°C for the amorphous reference. No discernable thermal event precedes the weak exotherm in the DSC trace of micronized materials; this feature in the micronized sample is clearly distinct from the  $T_g$  / recrystallization events observed for the amorphous reference. These results are consistent with those observed in the TSPC traces in that the disorder seen post-micronization is not comparable to the amorphous reference. Charmathy and Pinal (12) saw a comparable result in the case of Griseofulvin which displays a  $T_g$  at 88.7°C for the amorphous phase and a weak exothermic event occurring at a lower temperature (61°C) for a cryomilled sample. They observed a single relaxation in the milled sample via TSPC at ~56.4°C which appeared to potentially be associated with the DSC exotherm. Interestingly, for Felodipine, a  $T_g$  is observed at 41.6°C in the amorphous sample, and a weak exotherm at a slightly higher temperature of 45.5°C is seen in the milled sample. The first of two relaxations observed in the milled sample via TSPC displays a peak ~66°C. These collective observations suggest a complex series of physical processes associated with crystallization of crystal defects in organic systems.

Taken collectively, the data presented here are consistent with a disorder or defect system induced post micronization which is consistent with the “one-state model” as opposed to the “two-state model” (13,16). As such, we can envision the disordered regions to structurally contain a range of material from near true amorphous to longer range conformational disorder to material that is closer to crystalline in nature. Byard *et al.*, for example, have also discussed such continuum disorder resulting from the micronization of a developmental drug substance (13).



## Examining Material Micronized at Different Milling Energies

Drug substance samples prepared using different micronization energies were analyzed using the TSPC methodology described above. The total specific energy for the milling process is a function of the feed rate and the milling pressure. The energy range studied equated to approximately 90 to 430 kJ/kg, and 8 samples were generated through this range. In addition, a sample of non-micronized material is taken to represent drug substance with “0” micronization energy. Figure 8 displays normalized and background-corrected thermograms for the 9 samples examined in this study. The normalization procedure divides the TSPC current response by the sample area, applied electrical field, and sample mass to obtain a normalized dipolar conductivity. The final normalization step is background subtraction of the polarization peak to remove the current generated from crystalline material.

Examination of Fig. 8 shows that in general the responses (intensity or area under the curve (AUC)) associated with the  $\beta$ -relaxation are not resolved from each other with the exception of the response associated with the sample processed at 430 kJ/kg, which is clearly separated from the balance of the group. The onset of the  $\beta$ -relaxations are not impacted significantly by the change in micronization energy and appear around  $-40^\circ\text{C}$ , again with the exception of the high energy sample, which has a somewhat lower onset near  $-50^\circ\text{C}$ .

Responses associated with the  $\alpha$ -relaxation are more resolved as a function of micronization energy in the range studied. The onset of the features associated with the  $\alpha$ -relaxation remains basically constant with regard to micronization energy. As displayed in Fig. 8, both the peak intensity and AUCs appear to correlate reasonably with milling energy. Figure 9 demonstrates a linear response between milling energy and the normalized response

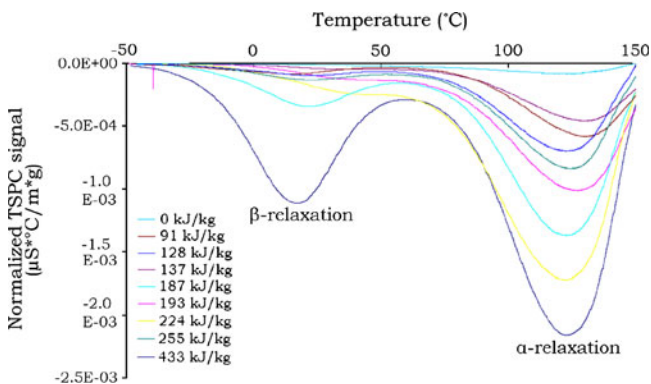


**Fig. 8** Normalized TSC spectra for Compound 1 processed at milling energies which range from 0 to 422 kJ/kg.

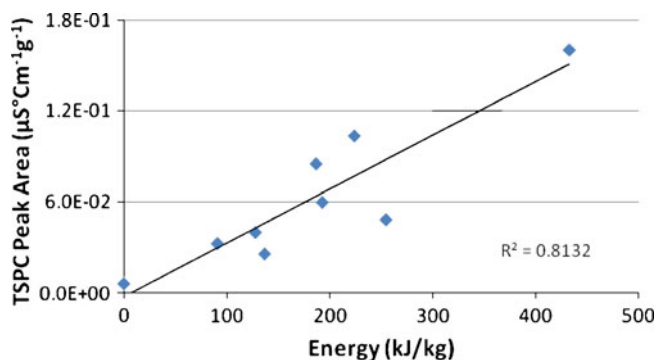


**Fig. 9** Plot of the linear correlation of the TSPC  $\alpha$ -relaxation peak area to milling energy (kJ/kg). A linear trend is observed, indicating an increase in defect density with higher milling energies.

associated with the  $\alpha$ -relaxation. Although the fit is not particularly strong ( $R^2=0.81$ ), it is clear that a trend between the intensity of the  $\alpha$ -relaxation and micronization energy is present in this range. This trend indicates that samples processed with increased micronization energy show an increased level of crystal defects. Also of note, there is no definitive evidence of the formation of phase-separated amorphous material at the higher milling energies. The results confirm that for the case of Compound 1, micronization generates non-crystalline regions which cannot be modeled as particles consisting of mixtures of purely amorphous and crystalline phases (16). Based on the data available here, it is difficult to confirm why the  $\alpha$ -relaxation may correlate better with micronization energy than the  $\beta$ -relaxation, and additional studies are needed to investigate this further.

## Annealing Process at Different Conditions

In order to further investigate the nature and behavior of the crystal defects observed in micronized Compound 1, stressing studies were performed. Material processed at 285 kJ/kg was stored under stressed and ambient conditions for up to 52 weeks to study the annealing process of the disorder in micronized materials. The samples were exposed directly to the conditions, i.e. open containers were used. The stressed conditions included  $40^\circ\text{C}$  with desiccant and  $40^\circ\text{C}$  75%RH. Samples were taken at the 2, 8, 24, and 52 (ambient only) week time-points and analyzed via the TSPC approach outlined above.

AUCs associated with the  $\beta$ - and  $\alpha$ -relaxations are calculated and contrasted against time for each of the conditions. Figures 10 and 11 show the area of the  $\alpha$ - and  $\beta$ -relaxation peaks over time for the micronized samples exposed to the different environmental conditions. The relaxation modes display trends in which temperature combined with moisture clearly impacts the overall inten-

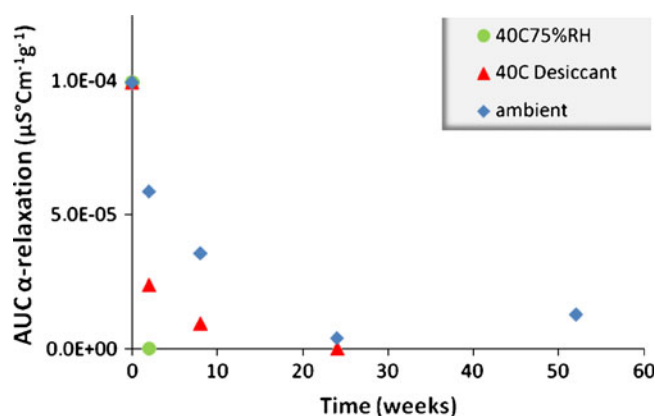


**Fig. 10** The AUC of the  $\alpha$ -relaxation peak over time for micronized Compound I stored at 40°C 75%RH, 40°C with desiccant, and ambient conditions for up to 52 weeks.

sity of the features. By 2 weeks storage at 40°C 75% RH, the  $\beta$ - and  $\alpha$ -relaxations are no longer detectable. This result indicates the noted conditions completely anneal the crystal defects associated with the TSPC signals. The observation that the rate of annealing of the crystal defects is enhanced by the presence of water vapor is not unexpected. The presence of sorbed water is well known to drive crystallization from the amorphous phase by increasing molecular mobility at a given temperature (17–19), although the impact on crystal defects is not as thoroughly studied. The observation also supports the proposal that the defects are associated with the particle surface (12,17). The crystalline form of Compound I investigated here is non-hygroscopic. Post-micronization the material remains non-hygroscopic, typically sorbing not more than 0.5% moisture between 0 and 90% RH at 25°C with no propensity to retain the water. These values are

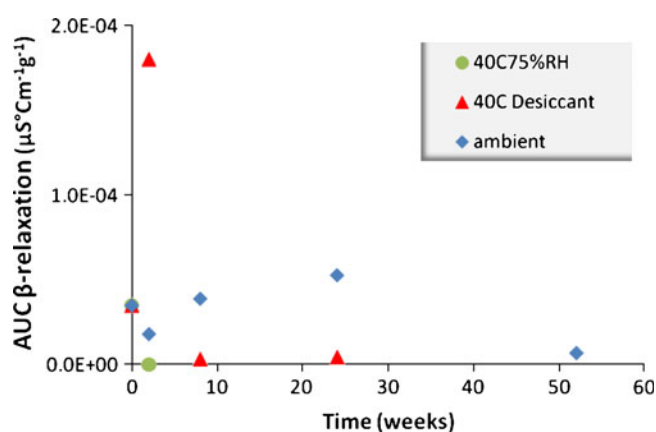


**Fig. 11** The AUC of the  $\beta$ -relaxation peak over time for micronized Compound I stored at 40°C 75%RH, 40°C with desiccant, and ambient conditions for up to 52 weeks. The apparent increase in intensity following the initial time point for the samples stored at 40°C with desiccant and ambient conditions is noted.

consistent with a surface adsorption process with no absorption into the bulk. In Fig. 12 we display an adsorption isotherm taken at 40°C to match the temperature of the annealing experiments. The exchanged moisture between 0 and 90% RH is  $\sim 0.3\%$ , and at 75% RH (the condition of the annealing) the value of moisture picked up is  $\sim 0.27\%$ . Based on analysis of the isotherm using the Guggenheim-deBoer equation, monolayer coverage occurs at approximately 45% RH ( $\sim 0.2\%$  mass increase). Again the data are consistent with a surface adsorption process, and this supports the view that the defect structure is closely associated with the particle surface. For the 40°C with desiccant and ambient conditions, the  $\beta$ - and  $\alpha$ -relaxations display different trends over time compared to those observed at 40°C 75% RH, and these are discussed in more depth below.

The  $\alpha$ -relaxation displays a consistent downward trend in which temperature and moisture clearly affect the TSPC mode over time. As noted, by 2 weeks storage at 40°C and 75% RH the  $\alpha$ -relaxation mode is not detected in the micronized sample. As displayed in Fig. 10 the elevated temperature alone (40°C with desiccant) shows a more gradual reduction in the  $\alpha$ -relaxation as compared to the 40°C 75% RH condition. A clear signal is still present at 8 weeks, but by 24 weeks, the  $\alpha$ -relaxation is no longer observed in the micronized materials. As expected, the slowest rate of annealing of the defect regions is observed in the material stored at ambient conditions. As shown in Fig. 10 a small but detectable signal is still present at 24 weeks, as well as 52 weeks. In both cases, the fall-off in intensities displays similar exponential decay-type shapes. The loss of the  $\alpha$ -relaxation appears to occur at a faster rate compared to the  $\beta$  mode based on the AUCs of the TSPC features.

Figure 11 shows the area of the  $\beta$ -relaxation peak over time for the micronized samples exposed to the stressed and ambient conditions. As mentioned above, the signal associated

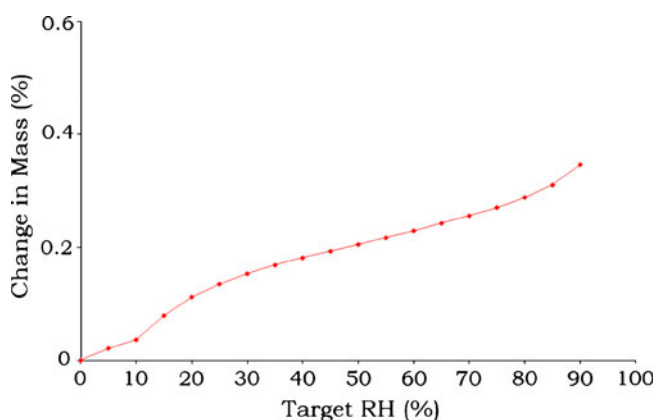


**Fig. 12** Sorption isotherm for micronized Compound I collected at 40°C using GVS. The data are consistent with a surface adsorption process.

with the  $\beta$ -relaxation is no longer detectable in micronized samples stored at 40°C 75%RH for 2 weeks. The samples stored at 40°C with desiccant show an apparent increase in the AUC for the  $\beta$ -relaxation at 2 weeks compared to the initial measurement, and then the mode becomes small but detectable at both the 8- and 24-week time-points. The ambient sample appears to demonstrate a similar trend, although to a lesser extent and at a slower rate, a slight increase in the AUC of the  $\beta$ -relaxation is indicated at weeks 8 and 24. Additionally, the  $\beta$ -relaxation peak shows a significantly reduced signal by 52 weeks. It is interesting to note that the  $\beta$ -relaxation appears to increase during the early part of the annealing process and then subsequently decreases in intensity. It appears that the kinetic mechanisms associated with the annealing of defects giving rise to the  $\beta$ - and  $\alpha$ -relaxation modes are distinct. A physical explanation for this observation cannot be derived from the results of this study; however, the observation does suggest the potential for additional studies in this area.

## CONCLUSIONS

In this paper we have reported on the use of TSC to study molecular mobility arising from crystal defects that are associated with the surface of micronized drug substance particles. Features observed in these samples are found to be distinct from those observed in amorphous reference materials. This confirms that for the case of Compound 1, micronization does not create phase-separated amorphous regions. TSC signals differentiate micronized drug substance processed using different milling energies. The AUC of the  $\alpha$ -relaxation correlates reasonably well against micronization energy, indicating the technique's ability to detect increased levels of crystalline defects for materials processed at higher energies. The annealing of disordered regions in micronized drug substance exposed to stressed and ambient environmental conditions was also studied. The kinetics of the annealing process of defect structures associated with the  $\alpha$ - and  $\beta$ -relaxation modes appear to be distinct, although more work is needed to fully explore this observation. This study suggests non-crystalline regions associated with crystal defects resulting from milling processes such as micronization possess interesting physical attributes and behavior which warrant additional investigation.

## ACKNOWLEDGEMENTS

The authors wish to thank Shadi Madieh for supplying the micronized samples processed at different milling energies. The authors also wish to thank the reviewers for constructive comments.

## REFERENCES

- Bhugra C, Pikal M. Role of thermodynamic, molecular, and kinetic factors in crystallization from the amorphous state. *J Pharm Sci.* 2008;97:1329–49.
- Shmeis RA, Wang Z, Krill S. A mechanistic investigation of an amorphous pharmaceutical and its solid dispersion, part I: a comparative analysis by thermally stimulated depolarization current and differential scanning calorimetry. *Pharm Res.* 2004;21:2025–30.
- Boutonnet-Fagegaltier N, Menegotto J, Lamure A, Duplaa H, Caron A, Lacabanne C, *et al.* Molecular mobility study of amorphous and crystalline phases of a pharmaceutical product by thermally stimulated current spectrometry. *J Pharm Sci.* 2002;91:1548–60.
- Alie J, Menegotto J, Cardon P, Duplaa H, Caron A, Lacabanne C, *et al.* Dielectric study of the molecular mobility and the isothermal crystallization kinetics of an amorphous pharmaceutical drug substance. *J Pharm Sci.* 2004;93:218–33.
- Shmeis RA, Wang Z, Krill S. A mechanistic investigation of an amorphous pharmaceutical and its solid dispersion, part II: molecular mobility and activation thermodynamic parameters. *Pharm Res.* 2004;21:2031–9.
- Vyazovkin S, Dranca I. Physical stability and relaxation of amorphous indomethacin. *J Phys Chem B.* 2005;109:18637–44.
- Correia NT, Moura Ramos JJ, Descamps M, Collins G. Molecular mobility and fragility in indomethacin: a thermally stimulated depolarization current study. *Pharm Res.* 2001;18:1767–74.
- Ediger MD, Angell CA, Nagel SR. Supercooled liquids and glasses. *J Phys Chem.* 1996;100:13200–12.
- Correia NT, Campos JM, Moura-Ramos J. Molecular motions in solid chloropentamethylbenzene: a thermally stimulated depolarisation currents study. *J Chem Soc, Faraday Trans.* 1997;93:157–63.
- Correia NT, Alvarez C, Moura Ramos JJ, Descamps M. Molecular motions in molecular glasses as studied by thermally stimulated depolarisation currents (TSDC). *Chem Phys.* 2000;252:151–63.
- Willart J, Lefebvre J, Danede F, Comini S, Looten P, Descamps M. Polymorphic transformation of the  $\Gamma$ -form of D-sorbitol upon milling: structural and nanostructural analyses. *Solid State Commun.* 2005;135:519–24.
- Chamarthy SP, Pinal R. The nature of crystal disorder in milled pharmaceutical materials. *Colloids and Surfaces A.* 2008;331:68–75.
- Byard S, Jackson S, Smail A, Bauer M, Apperley D. Studies on the crystallinity of a pharmaceutical development drug substance. *J Pharm Sci.* 2004;94:1321–35.
- Bates S, Zografi G, Engers D, Morris K, Crowley K, Newman A. Analysis of amorphous and nanocrystalline solids from their X-ray diffraction patterns. *Pharm Res.* 2006;23:2333–49.
- Venkatash G, Barnett M, Owusu-Fordjour C, Galop M. Detection of low levels of the amorphous phase in crystalline pharmaceutical materials by thermally stimulated current spectroscopy. *Pharm Res.* 2001;18:98–103.
- Rani M, Govindarajan R, Surana R, Suryanarayanan R. Structure in Dehydrated Trehalose Dihydrate – Evaluation of the Concept of Partial Crystallinity. *Pharm Res.* 2006;23:2356–67.
- Ward GH, Schultz RK. Process-induced crystallinity changes in albuterol sulfate and its effect on powder physical stability. *Pharm Res.* 1995;12:773–9.
- Ahlneck C, Zografi G. The molecular basis of moisture effects on the physical and chemical stability of drugs in the solid state. *Int J Pharm.* 1990;62:87–95.
- Burnett DJ, Thielmann F, Sokoloski T, Brum J. Investigating the moisture-induced crystallization kinetics of spray-dried lactose. *Int J Pharm.* 2006;26:23–8.